CIGRE-US National Committee

2023 Next Generation Network Paper Competition

Powering the Future: Harnessing Neural Dynamic Equivalence for Enhanced Power System Applications

Q. SHEN[1], Y. ZHOU[1], H. ZHAO[1], P. ZHANG[1], Q. Zhang[2], S. Maslennikov[2], X. Luo[2]

Member ID: 920220194

Research assistant

1. Stony Brook University
2. ISO New England

Professionals with Less than Ten Years of Experience

qing.shen@stonybrook.edu, yifan.zhou.1@stonybrook.edu, qzhang@iso-ne.com

SUMMARY

Traditional grid analytics are model-based, relying strongly on accurate models of power systems, especially the dynamic models of generators, controllers, loads and other dynamic components. However, acquiring thorough power system models can be impractical in real operation due to inaccessible system parameters and privacy of consumers, which necessitate data-driven dynamic equivalencing of unknown subsystems. Learning reliable dynamic equivalent models for the external systems from SCADA and PMU data, however, is a long-standing intractable problem in power system analysis due to complicated nonlinearity and unforeseeable dynamic modes of power systems.

This paper advances a practical application of neural dynamic equivalence (NeuDyE) called Driving Port NeuDyE (DP-NeuDyE), which exploits physics-informed machine learning and neural-ordinary-differential-equations (ODE-NET) to discover a dynamic equivalence of external power grids while preserving its dynamic behaviors after disturbances. The new contributions are threefold:

- A NeuDyE formulation to enable a continuous-time, data-driven dynamic equivalence of power systems, saving the effort and expense of acquiring inaccessible system;
- An introduction of a Physics-Informed NeuDyE learning (PI-NeuDyE) to actively control the closed-loop accuracy of NeuDyE; and
- A DP-NeuDyE to reduce the number of inputs required for the training.

We conduct extensive case studies on the NPCC system to validate the generalizability and accuracy of both PI-NeuDyE and DP-NeuDyE, which span a multitude of scenarios, differing in the time required for fault clearance, the specific fault locations, and the limitations of data. Test results have demonstrated the scalability and practicality of NeuDyE, showing its potential to be used in ISO and utility control centers for online transient stability analysis and for planning purposes.

KEYWORDS

Neural dynamic equivalence, ODE-NET, physics-informed machine learning, model order reduction, driving port.

1. INTRODUCTION

Reliable discovery of dynamic equivalent models for unidentified subsystems, specifically external systems, is crucial to ensure reliable operations of large-scale interconnected transmission systems [1]. However, this task has been a longstanding challenge due to the existence of nonlinear dynamics, complex coherency characteristics, and unavailable component models [2, 3]. Recent advancements in Phasor Measurement Units (PMUs) provide an opportunity to readily obtain rich history of high-data-rate measurements, which fostered the development of data-driven dynamic equivalence [4]. Despite various attempts being reported in the literature, significant challenges persist: (I) Learning continuous-time dynamic behaviors using discrete-time measurements is difficult. Traditional discretization techniques may not fully capture the intricacies of the continuous dynamics, leading to large inaccuracies that limit its practical implementations. (II) Achieving robust and stable closed-loop operations under diverse operating conditions and disturbances is essential for safe plug-and-play integration of dynamic equivalence. Whereas none of the existing dynamic equivalencing methods have achieved successful closed-loop operations with bulk power grid models. (III) The final challenge lies in minimizing the required measurements to ensure a feasible and practical implementation.

This research makes three significant contributions to address the aforementioned challenges:

- Formulation of Ordinary Differential Equations (ODEs)-Net-enabled Dynamic Equivalence (NeuDyE): It leverages ODEs and neural networks to model the system dynamics, providing a continuous-time, data-driven representation that aligns with the actual behavior of power grids.
- Introduction of Physics-Informed Neural Dynamic Equivalence (PI-NeuDyE): It combines an ODE-NET-enabled equivalent model with a physics-informed learning to identify a continuous-time dynamic equivalence while ensuring the closed-loop dynamic behaviors under disturbances.
- Implementation of a Driving Port NeuDyE (DP-NeuDyE): It reduces the number of inputs required for training, making it more manageable and cost-effective to deploy in real-world interconnected bulk power systems.

2. PROBLEM FORMULATION

For a reliability coordinator (RC), the entire interconnection can be partitioned into an internal system (InSys) and the external systems (ExSys). Take the 140-bus NPCC system as an example, InSys and ExSys, connected through two tie lines [5], are illustrated in Figure 1.

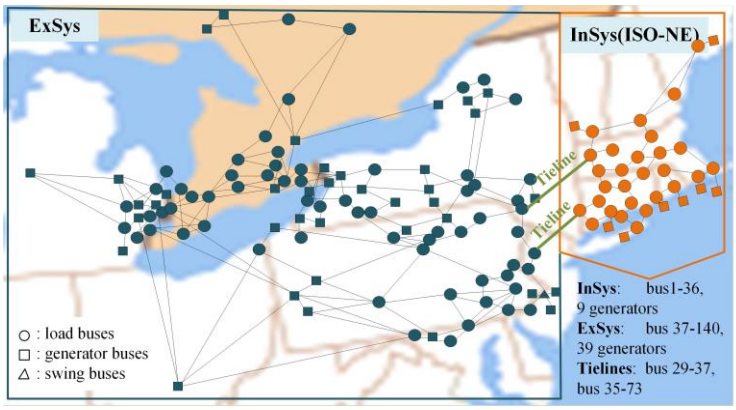

Figure 1 Topology of the NPCC system

InSys (buses 1-36), which is the simplified ISO New England (ISO-NE) system, represents the subsystem that can be characterized by precise knowledge of its structure and parameters, enabling straightforward formulation using dynamic models. InSys can be formulated based on the known dynamics of components by a set of differential algebraic equations (DAEs).

In contrast, ExSys (buses 37-140) lacks accessible physics models due to factors such as unavailable system state measurements, privacy concerns and inaccessible local measurements, e.g., real-time dispatch of the generators. Therefore, a data-driven neural network based dynamic equivalence is relied upon to model ExSys, as in (0.1) [6]:

$$\frac{dx_{in}}{dt} = \mathcal{P}(x_{in}, y_{in}, i_{tie});\ G(x_{in}, y_{in}, i_{tie}) = 0;\ \frac{dx_{ex}}{dt} = \mathcal{N}(x_{ex}, z_{in}) \tag{0.1}$$

Here, x_{in} denotes the state variables of InSys's components (e.g., generators, exciters); y_{in} denotes the algebraic variables of InSys such as power flow states; i_{tie} denotes the tie line currents. Functions $\mathcal{P}$ and G denote the dynamic and algebraic equations of InSys, respectively, which can be readily established based on the physics models of InSys. x_{ex} denotes the state variables of ExSys; z_{in}

denotes the features from InSys, which is selected from part of InSys states to describe the interaction between InSys' dynamics and ExSys' dynamics. $\mathcal{N}$ is the forward propagation function of a neural network, which mimics the ExSys dynamics. Neural network-enabled dynamic equivalence is flexible for approximating a dynamic system without requiring the system to be linear or assuming any dynamical modes beforehand.

3. ODE-NET-ENABLED DYNAMIC EQUIVALANCE

3.1 PHYSICS-INFORMED CONTINOUS-BACKPROGATION

A neural network (NN) is a nonlinear function with parameters that are optimized by minimizing a loss function, typically computed as the error between measurements and NN outputs. However, in this problem, the challenge is that the NN's output is a derivative $\dot{x}_{ex}$ while the measurements provide only direct values x_{ex}. Two approaches exist: discrete-time learning and continuous-time learning. Discrete-time learning discretizes the continuous-time differential equations into discrete-time difference equations. It is sensitive to derivative estimation, resulting in biased training outcomes due to residue errors during training. Although it may produce satisfactory derivatives fitting, it cannot guarantee the accuracy of system states after numerical integration.

ODE-NET training is different since it involves numerical integration in its constraints. It directly minimizes the difference between real dynamic states and trained dynamic states, which requires no discretization and fully respects the continuous-time characteristics of power system dynamics. By introducing an adjoint method [7, 8] to remove the numerical integration constraints, a physic-informed (PI) continuous-backpropagation is developed:

$$\begin{aligned}
&\min_\theta \sum_{i=0}^{n} L(x_{ex,i}, x_{in,i}) = \sum_{i=0}^{n} \frac{\eta_i}{2}(\| x_{ex,i} - x_{ex,i} \|_2 + \| x_{in,i} - x_{in,i} \|_2) \\
&\mathcal{L} = \sum_{i=0}^{n} L_i - \int_{t_0}^{t_n} \left[\lambda^T (\dot{x}_{ex} - \mathcal{N}_\theta) + \mu^T (\dot{x}_{in} - \tilde{\mathcal{P}}) \right] dt \\
&s.t.\ x_{ex,i} = x_{ex,0} + \int_{t_0}^{t_i} \mathcal{N}(x_{ex}, z_{in}, \theta) dt,\ x_{in,i} = x_{in,0} + \int_{t_0}^{t_i} \mathcal{P}(x_{in}, y_{in}, i_{tie}) dt
\end{aligned} \tag{0.2}$$

where λ and μ respectively denote the adjoint states for ExSys and InSys, $\tilde{\mathcal{P}}$ is equivalently formulated from $\mathcal{P}$ using (0.1). $\mathcal{N}$ is an ODE-Net parameterized by θ. The dynamics of InSys and ExSys are both considered in (0.2), which assures the performance of ODE-NET in the closed-loop simulation of the whole power system. With proper adjoint boundary conditions [8], the physics-informed gradient is:

$$\frac{d}{dt}\begin{bmatrix} \lambda^T \\ \mu^T \\ \partial\mathcal{L}/\partial\theta \end{bmatrix} = \begin{bmatrix} -\lambda^T \partial\mathcal{N}/\partial x_{ex} - \mu^T \partial\tilde{\mathcal{P}}/\partial x_{ex} \\ -\lambda^T \partial\mathcal{N}/\partial x_{in} - \mu^T \partial\tilde{\mathcal{P}}/\partial x_{in} \\ \lambda^T \partial\mathcal{N}/\partial\theta \end{bmatrix},\ \theta \leftarrow \theta - \frac{\partial\mathcal{L}}{\partial\theta} \tag{0.3}$$

Finally, the gradient descent for $\mathcal{N}_\theta$ can be performed using $\partial\mathcal{L}/\partial\theta|_{t=0}$ integrated from (0.3).

3.2 NETWORK EQUIVALENT SEEN FROM DRIVING PORT

In the previously devised PI-NeuDyE, the optimal closed-loop results are achieved using extensive inputs from the internal system, which may not be readily available in practical applications. To make the method applicable in such scenarios, we develop an enhanced neural equivalent technique called the Driving Port NeuDyE (DP-NeuDyE) which only needs boundary voltages v_p for the tie-lines, empowering the practical implementations of NeuDyE in utilities and ISOs.

3.3.1 Algebraic component separation

If ExSys is static, a Norton equivalent current source, depicted in Figure 2(b), can replace it. From the perspective of InSys, the representation of ExSys in full detail or as a Norton equivalent current source yields the same output i_{tie} for the given input v_p. Inspired by the Norton equivalent theory, we

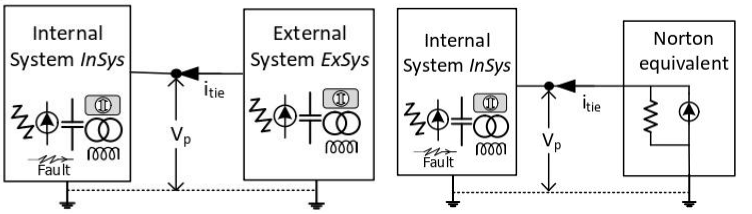

(a) Original networks (b) Norton equivalent

Figure 2 Network equivalent methodology

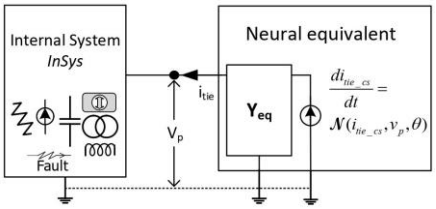

Figure 3 TSA interface for NeuDyE

develop a neural network observed from the driving port. To capture its nonlinear dynamics, measurements of port voltages v_p and tie currents i_{tie} are utilized to discover the state space model of ExSys as shown in Figure 2(b). The tie currents i_{tie} are selected as the state variables for external system x_{ex}, whose continuous differential structure is represented by the neural network; then a magic touch, the algebraic component separation, is introduced bellow:

$$\frac{di_{tie}}{dt} = \mathcal{N}(i_{tie}, v_p, \theta);\ \mathcal{G}(i_{tie}, v_p) = 0;\ i_{tie} = C_s \cdot x_{ex} + D \cdot v_p \tag{0.4}$$

where the port voltages v_p corresponds to the InSys features z_{in} in (0.1). The tie currents i_{tie} is represented as a linear combination of state variables and inputs. Here matrices C_s and D are constant matrices. If a fault happens in the internal network at time instant t_i, sudden changes may happen in $\Delta v_p(t_i) = v_p(t_i + \Delta t) - v_p(t_i)$, while $x_{ex}(t_i)$ keeps invariant in a very short period of Δt, i.e. $\Delta x_{ex}(t_i) = 0$. The components i_{tie} can be split into two types of components: continuous-state-variable components $i_{tie\_cs} = C_s \cdot x_{ex}$ and algebraic components $i_{tie\_a} = D \cdot v_p$. Algebraic components embody the port voltages v_p, which may exhibit discontinuity during switching events within the internal network. On the other hand, continuous-state-variable components, i_{tie_cs}, are employed as the constituents of the neural network equivalent as in equation (0.4). These components fulfill the need for continuity as depicted in equation (0.4). To compute the coefficient matrix D, we leverage measurement data obtained during the fault period. This is achieved by using the least squares method:

$$\begin{bmatrix} D_{11} & \cdots & D_{1n_p} \\ \vdots & \ddots & \vdots \\ D_{n_p 1} & \cdots & D_{n_p n_p} \end{bmatrix} = \left[\Delta i_{tie}(t_1), \quad \cdots, \quad \Delta i_{tie}(t_{n_f})\right] \cdot \left[\Delta v_p(t_1), \quad \cdots, \quad \Delta v_p(t_{n_f})\right]^{-1} \tag{0.5}$$

where n_p is the number of port voltages, n_f is the number of faults whose port voltages and tie line currents are in the data sets. Define $\Delta v_p(t_i) = v_p(t_i + \Delta t) - v_p(t_i)$ and $\Delta i_{tie}(t_i) = i_{tie}(t_i + \Delta t) - i_{tie}(t_i)$. The continuous component $i_{tie\_cs} = i_{tie} - D \cdot v_p$. The neural equivalent network in (0.4) and the DAE now become:

$$\frac{di_{tie\_cs}}{dt} = \mathcal{N}(i_{tie\_cs}, v_p, \theta);\ \frac{dx_{in}}{dt} = \mathcal{P}(x_{in}, y_{in}, i_{tie});\ \mathcal{G}(x_{in}, y_{in}, i_{tie\_cs}, i_{tie}, v_p) = 0 \tag{0.6}$$

The neural equivalent of the external system and the corresponding formulated interface as shown in Figure 3 are integrated into Transient Stability Analysis (TSA) simulation. The values of current sources are updated by applying an explicit integration method to (0.6). During the time interval from $0 \sim t_n$, ODE-NET is trained by minimizing the loss function defined by the error between the state measurements $\hat{i}_{tie\_cs}$ and the numerical solution i_{tie_cs} by (0.6), and similar as in (0.3), ODE-NET computes gradients using the adjoint sensitivity method :

$$L=\sum_{i=0}^{n}\frac{1}{2}\|\, i_{tie\_cs}(t_i)-\hat{i}_{tie\_cs}(t_i)\,\|_2,\ i_{tie\_cs}(t_i)=\hat{i}_{tie\_cs}(0)+\int_0^{t_i}\mathcal{N}(x,u,\theta)dt$$

$$\frac{d}{dt}\begin{bmatrix}a^T\\ \partial L/\partial\theta\end{bmatrix}=\begin{bmatrix}-a^T\cdot\dfrac{\partial\mathcal{N}}{\partial i_{tie\_cs}}\\ a^T\cdot\dfrac{\partial\mathcal{N}}{\partial\theta}\end{bmatrix},\ a=\partial L/\partial i_{tie\_cs} \tag{0.7}$$

3.3.3 Strengthening ODE-NET Based on Recurrent Neural Network

Data-driven methodologies predominantly depend on observable states to construct the neural equivalent model, as exemplified in equation (0.4). However, this model reduction approach inherently leads to a scenario where state variables constitute only a minor subset of the comprehensive state variables present in the original power network. As a result, such a reduction may not entirely encapsulate all the crucial dynamic properties intrinsic to the power system.

To address this deficiency of information, we enhance DP-NeuDyE in this section by leveraging historical data through the implementation of Recurrent Neural Networks (RNNs) [9]. RNNs, with their unique ability to remember past information, provide a robust mechanism to incorporate temporal dynamic behavior into the model. The integration of RNNs into the DP-NeuDyE framework is explained as follows. The differential term di_{tie_cs}/dt can be represented as:

$$\frac{di_{tie\_cs}}{dt}=\lim_{\delta\to 0}\frac{i_{tie\_cs}(t)-i_{tie\_cs}(t-\delta)}{\delta}\approx\frac{i_{tie\_cs}(t)-i_{tie\_cs}(t-\Delta t)}{\Delta t} \tag{0.8}$$

where Δt denotes a short period of time. Equation (0.8) implies that the historical information at time instant $t-\Delta t$ could help determine the derivative at time instant t. Recall that the continuous backpropagation for ODE-NET in 3.3.2 already considers integration along the time by solving an augmented differential equation. Therefore, the backward propagation throughout time for the RNN cell is ignored and the gradient descent method used in 3.3.2 can directly be applied to the RNN-empowered ODE-NET. As illustrated in Figure 4, the structure of the RNN cell integrates the output of a specific neuron from the previous time step into the computation of the current time step's output for the same neuron. This mechanism effectively leverages historical data from the preceding time step to assist in calculating the derivative of the current time step. Therefore, this approach ameliorates potential information deficiencies that might arise when computations rely on a limited subset of state variable, thereby bolstering the overall accuracy and robustness of DP-NeuDyE.

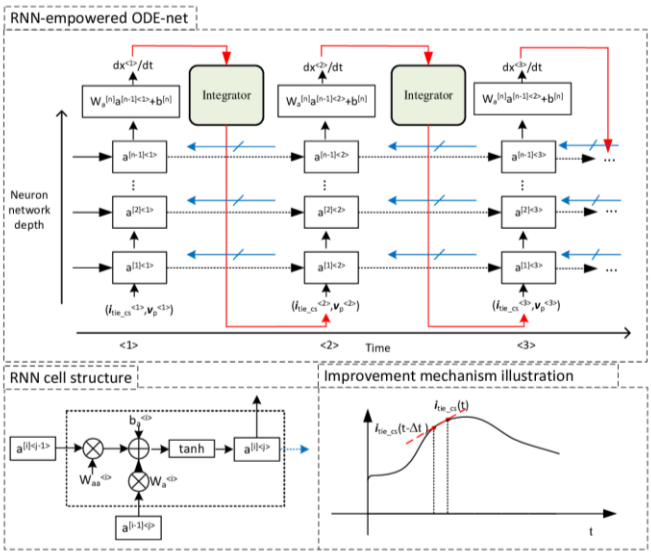

Figure 4 RNN empowered ODE-NET

4. CASE STUDY

In this section, the detailed training and testing procedures of NeuDyE are introduced. Simulation results of PI-NeuDyE and DP-NeuDyE are presented to demonstrate their efficacy and practicality.

4.1 TRAINING DETAIL

The ground truth electromechanical trajectories are obtained by simulating the complete, physics-based 140-bus NPCC system via the Power System Toolbox (PST). The PST results are verified with

simulations from Transient Security Assessment Tool (TSAT). Trapezoidal rule is adopted as the numerical integration method for the devised method.

4.1.1 Open-loop, data-driven ODE-NET Training

PI-ODE-NET: as introduced in Subsection 3.2.2, the selected states are from generators, exciters, governors, and line currents of InSys as s_{in}, in total 90 dimensions; the tie line currents are the states of ExSys x_{ex} with 4 dimensions (2 tie lines, each has a real part and an imaginary part).

RNN-empowered DP-ODE-NET: followed by 3.3, s_{in} includes boundary voltages with 4 dimensions (2 ports with real parts and imaginary parts); x_{ex} consists of tie line currents; as such, DP-ODE-NET is faster than PI-ODE-NET. However, this comes at the expense of compromising the model's generalization ability, resulting in less accurate predictions for unseen scenarios.

4.1.2 Closed-Loop Testing

After an ODE-NET is obtained, the closed-loop tests check its performance. Closed-loop means the ODE-NET-based ExSys model replaces the unknown subsystems and integrates with the physics-based InSys model. This is the final setup. The entire system's dynamics are then computed through numerical integration. The predicted values are trajectories simulated by the physics-neural-integrated system, containing physics-based InSys and the ODE-NET-based dynamic equivalence of the ExSys.

4.2 SIMULATION RESULTS

4.2.1 Varied fault clearing times and fault locations using PI-NeuDyE

25 training scenarios are generated by launching three-phase faults at 0.50s at buses 18, 19, 20, 21, or 28 with fault clearing set randomly within a time interval [0.53s, 0.6s]. The training variables of InSys have 90 dimensions as mentioned in 4.1.1. Figure 5 shows the schematic diagram of PI-NeuDyE and the test results on buses 1, 32, 16 with faults cleared at 0.54s, 0.56s, and 0.58s, respectively, which are new clearing times and locations to the training sets. Trajectories of boundary voltage of bus 35 demonstrate a perfect match between PI-NeuDyE's results and that from the full NPCC model, showing that it can accurately represent the dynamics regardless of changes in fault durations or fault locations.

Further, in Figure 6, 108 testing scenarios are generated with new fault locations and random fault clearing times at buses 2, 5, 9, 16, 25, 28, 32, 34 and 35. The box plot shows that the overall relative error is lower than 1%, indicating a satisfying generalization ability.

4.2.2 Reduced variables using DP-ODE-NET

As previously mentioned, DP-NeuDyE is designed for potential practical applications that require limiting the number of input variables. In contrast with 4.2.1, DP-NeuDyE only needs 4 dimensions of InSys features instead of 90. The selections of ExSys features are the same for both methods. This model in Figure 7 is derived from five distinct dynamic trajectories, each triggered by phase-to-ground faults at the T-line, as highlighted in red. In the testing, the low-frequency oscillation is initiated by a phase-to-ground fault located at the green circle. It can be observed that DP-NeuDyE is able to precisely predict the low frequency oscillations in a fairly large area. Since the testing faults are not in the training set (historical record), the predictability of the proposed method is validated. Besides, there are two oscillation modes in the full model-based trajectory: 0.5991 Hz with a magnitude of 0.2155 and 1.24813 Hz with a magnitude of 0.1349. The neural equivalent model-based simulation also accurately predicts those oscillation modes, with a magnitude of 0.2051 and 0.1431 respectively.

4.2.3 Generalizability analysis based on electrical distance

To quantify the NeuDyE models' generalization performance, we employ the electrical distance between the fault locations in the testing set and those in the training set as a measure. The network topology is transformed into an adjacency matrix using graph theory, as depicted in equation (0.9). Consequently, the electrical distance between a new fault location and those in the training set can be determined from the adjacency matrix by selecting the shortest distance.

$$\text{Ajacency matrix } A:\begin{cases}\text{Electric connection between BUS i and j: } A_{ij}=X_{ij}\\ \text{Else: } A_{ij}=0\\ \text{Fault dynamic record near BUS i: } A_{ii}=1\end{cases} \tag{0.9}$$

where $i \neq j$ and X_{ij} is the reactance (p.u.) in the branch connecting $BUS\ \ i$ and j.

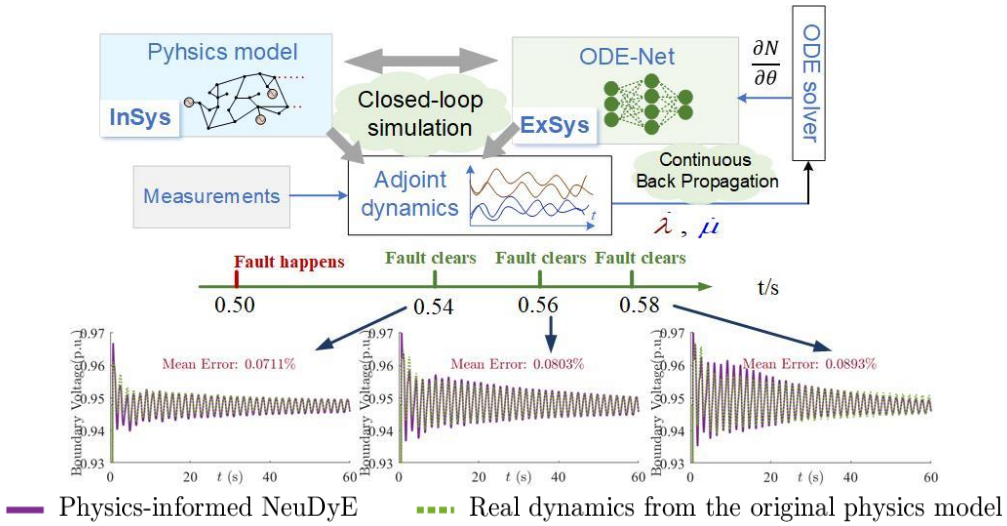

Figure 5 Closed-loop test results of fault with different locations

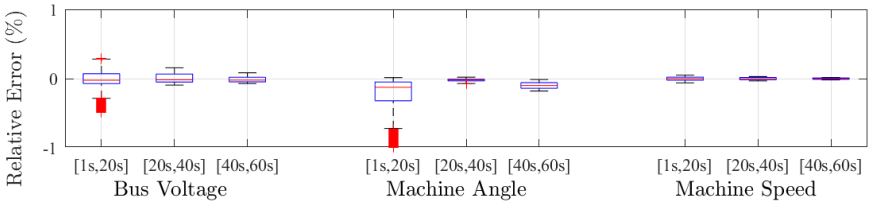

Figure 6 Accuracy of PI-NeuDyE under 108 cases with new fault locations and random clearing times

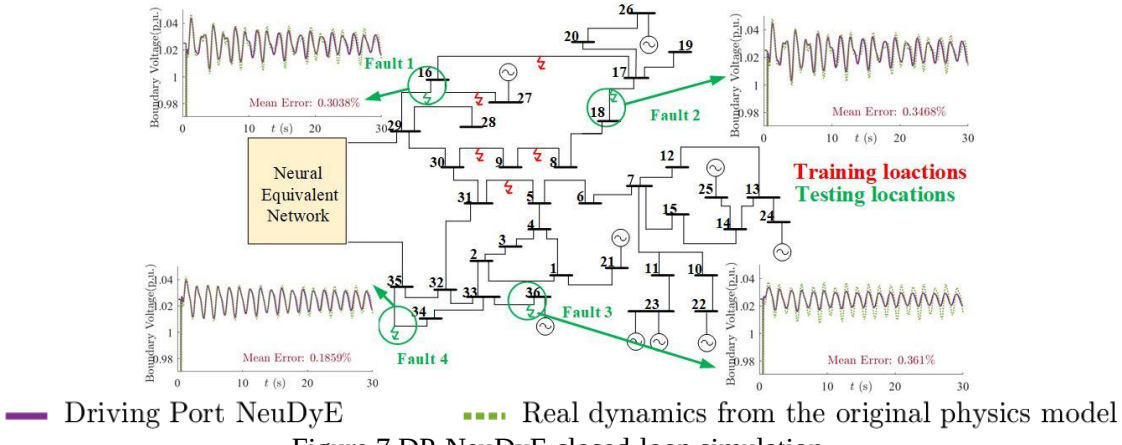

Figure 7 DP-NeuDyE closed-loop simulation.

In the previous case study as depicted in Figure 7, the electrical distances from the test set to the training set are as follows: 0, 0.0255, 0.0404, 0.0369. These electrical distances are relatively small; the generalizability of the DP-NeuDyE is thus relatively good. However, if a fault occurs distantly, such as the T-line between buses 19 to 17, where the electrical distance is 0.0948, DP-NeuDyE may encounter challenges in making accurate dynamic predictions, as illustrated in Figure 8(a).

That is exactly when RNN-empowered ODE-NET shows its advantage of a better generalization ability. For the same training set and testing scenario, the trajectory by the RNN-empowered neural equivalent model is shown in Figure 8(b), which achieves convergence.

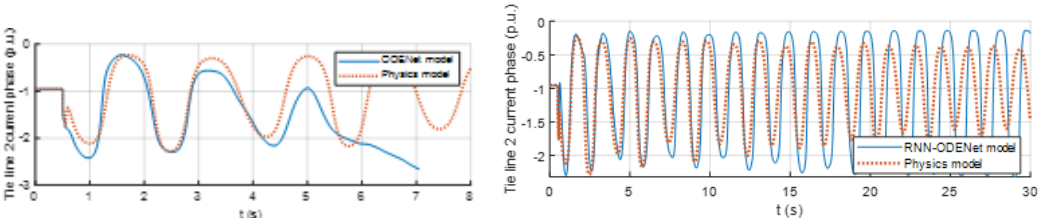

(a) Erroneous prediction (b) RNN empowered model prediction

Figure 8 RNN-empowered DP-ODE-NET simulation

However, its performance is still not as commendable as PI-NeuDyE (results are omitted due to space). The primary reason behind this discrepancy lies in the training process. PI-NeuDyE trains in a closed-loop manner by considering the interacting dynamics of both InSys and ExSys, involving 90 dimensions of InSys features. Whereas DP-NeuDyE only sees from the driving port, utilizing only 4 dimensions of boundary measurements as InSys features. As a result, there exists a trade-off between training efficiency and generalization ability, which impacts the overall performance of the DP-NeuDyE. For fault not too distant from the training sets, both DP-NeuDyE and PI-NeuDyE yield satisfactory results.

5. CONCLUSION

This article introduces a physics-integrated Neural Dynamic Equivalence (PI-NeuDyE) and its practical application Driving Port NeuDyE (DP-NeuDyE), which uncovers a powerful continuous-time dynamic equivalence of external systems. One of its key advantages is the ability to preserve the continuous-time dynamic characteristics of power grids while using fewer variables. The effectiveness of DP-NeuDyE and PI-NeuDyE are demonstrated through case studies conducted on the 140-bus NPCC system, showcasing their performance under various fault locations and clearing times. Furthermore, comparisons are made between DP-NeuDyE and PI-NeuDyE in terms of efficiency and generalization ability.

BIBLIOGRAPHY

[1] M. L. Ourari, L.A. Dessaint, and V.-Q. Do, “Dynamic equivalent modeling of large power systems using structure preservation technique,” IEEE Transactions on Power Systems, vol. 21, no. 3, pp. 1284–1295, 2006.

[2] Y. G. I. Acle, F. D. Freitas, N. Martins, and J. Rommes, “Parameter preserving model order reduction of large sparse small-signal electrome- chanical stability power system models,” IEEE Transactions on Power Systems, vol. 34, no. 4, pp. 2814–2824, 2019.

[3] I. Tyuryukanov, M. Popov, M. van der Meijden, and V. Terzija, “Slow coherency identification and power system dynamic model reduction by using orthogonal structure of electromechanical eigenvectors,” IEEE Transactions on Power Systems, vol. 36, no. 2, pp. 1482–1492, 2020.

[4] N. Tong, Z. Jiang, S. You, L. Zhu, X. Deng, Y. Xue, and Y. Liu, “Dynamic equivalence of large-scale power systems based on boundary measurements,” in 2020 American Control Conference (ACC), pp. 3164– 3169, IEEE, 2020.

[5] Y. Lei, Y. Liu, G. Kou, B. Wang, "A study on wind frequency control under high wind penetration on an NPCC system model," 2014 IEEE PES General Meeting, National Harbor, MD, USA, 2014, pp. 1-5.

[6] Q. Shen and Y. Zhou, “Physics-Aware Neural Dynamic Equivalence of Power Systems,” IEEE Transactions on Power Systems, under review.

[7] Y. Zhou and P. Zhang, “Neuro-reachability of networked microgrids,” IEEE Transactions on Power Systems, vol. 37, no. 1, pp. 142–152, 2022.

[8] R. T. Q. Chen, Y. Rubanova, J. Bettencourt, and D. K. Duvenaud, “Neural ordinary differential equations,” vol. 31, 2018.

[9] D. E. Rumelhart, G. E. Hinton, and R. J. Williams, “Learning representations by back-propagating errors,” nature, vol. 323, no. 6088, pp. 533–536, 1986. 19.